

# Non-transcriptional regulatory processes shape transcriptional network dynamics

J. Christian J. Ray\*<sup>‡</sup>, Jeffrey J. Tabor\* and Oleg A. Igoshin\*

**Abstract** | Information about the extra- or intracellular environment is often captured as biochemical signals that propagate through regulatory networks. These signals eventually drive phenotypic changes, typically by altering gene expression programmes in the cell. Reconstruction of transcriptional regulatory networks has given a compelling picture of bacterial physiology, but transcriptional network maps alone often fail to describe phenotypes. Cellular response dynamics are ultimately determined by interactions between transcriptional and non-transcriptional networks, with dramatic implications for physiology and evolution. Here, we provide an overview of non-transcriptional interactions that can affect the performance of natural and synthetic bacterial regulatory networks.

## Networks

Sets of biochemical reactions or interactions that are employed for information processing in the cell. The term network can refer to either interactions on the whole-cell level or smaller circuits (subsystems) within the larger network.

## Signal

In the context of this Review, the information that flows through a biological network. In a wider context, biological signals can take a variety of forms.

Regulatory networks determine how cells adapt to the extra- or intracellular environment. In a typical network, a sensor detects a physical or chemical stimulus and transmits that information into the network as a biochemical signal. Networks are composed of a series of interconnected nodes, or signal-processing molecules (FIG. 1a). Each node receives an input signal from an upstream node and sends an output signal to a downstream node in response.

Signals often flow through hierarchically structured transcriptional networks, in which each node is a transcription factor<sup>1,2</sup>. The final output of the network is a set of induced or repressed genes that determines the phenotype of the cell in response to information flowing through the network. Within these networks are many smaller modules with certain over-represented structural features, such as feedback or feedforward loops, that may carry specific physiological functions<sup>3,4</sup>. Despite thorough studies on the properties of these transcriptional regulatory motifs<sup>5–8</sup>, connectivity maps of transcriptional networks alone are often insufficient to explain the dynamic response of a cell to a given stimulus. A wide range of non-transcriptional interactions — post-transcriptional, post-translational and pleiotropic processes — can affect the functionality of transcriptional networks. Indeed, non-transcriptional signal processing can result in a complex network diagram even when only one or a handful of genes are involved. Only by viewing transcriptional networks along with the mechanistic

details of their associated non-transcriptional processes can we arrive at a complete understanding of cellular regulation.

Non-transcriptional processes such as phosphorylation, methylation, regulated degradation of proteins and mRNA, and sequestration can have unexpected consequences in regulatory networks. Consider a bacterial two-component system (FIG. 1b). A bifunctional sensor with both kinase and phosphatase activity senses an environmental stimulus and modulates the fraction of activated response regulator, which in turn modulates transcription of a downstream regulon<sup>9</sup>. The transcriptional network diagram of a typical two-component system is simple (FIG. 1b, lower panel): the sensor and response regulator genes are expressed from a positively autoregulated operon<sup>10</sup>. However, an apparently minor non-transcriptional detail — whether the response regulator undergoes a low level of non-cognate sensor kinase-mediated phosphorylation — can drastically alter the effect of the feedback on the dynamic response<sup>11</sup> (FIG. 1c). Such non-cognate phosphorylation can come either from crosstalk with other sensor kinases or from phosphotransfer from small molecules. This effect constitutes a small fraction of the total phosphorylation flux when the system is activated, and it is buffered by sensor phosphatase activity to prevent activation of the system in the absence of signal input<sup>11</sup>. Nonetheless, this slight difference in phosphorylation changes the dynamic behaviour of the system in an important way.

\*Department of Bioengineering, Rice University, 6100 Main St., Houston, Texas 77005, USA.

<sup>‡</sup>Department of Systems Biology, The University of Texas MD Anderson Cancer Center, Houston, Texas 77030, USA.  
Correspondence to O.A.I.  
e-mail: igoshin@rice.edu  
doi:10.1038/nrmicro2667  
Published online  
11 October 2011

**Nodes**

Molecular entities, such as transcription factors or allosterically regulated enzymes, that take in a signal and then output a signal in response. When a node is described as upstream or downstream, this refers to its order in the information flow.

**Pleiotropic**

Of an interaction: in which one component or effect simultaneously affects many targets. In this Review, we refer to effects originating from coupling with global physiological processes in the cell.

**Ultrasensitivity**

A type of signal–response curve characterized by a high slope in the responsive range.

**Michaelis–Menten kinetics**

A model of enzyme kinetics that is often used to mathematically represent first-order saturation processes, in which the flux ( $V$ ) is determined by the equation:  

$$V = V_{\max} \frac{[x]}{K_m + [x]}$$
 (in which  $[x]$  is the concentration of substrate or regulator  $x$ ,  $V_{\max}$  is the maximum flux rate and  $K_m$  is the Michaelis–Menten constant).

**Hill kinetics**

A generalization of Michaelis–Menten kinetics that allows a mathematical representation of higher-order, or cooperative, processes in which the flux

$$V = V_{\max} \frac{[x]^n}{K_m^n + [x]^n}$$

has  $n^{\text{th}}$ -order effective cooperativity ( $[x]$  is the concentration of substrate or regulator  $x$ ,  $V_{\max}$  is the maximum flux rate,  $K_m$  is the Michaelis–Menten constant and  $n$  is the Hill coefficient).

**Effective cooperativity**

A measure of sensitivity: how much one molecular species affects the production of another.

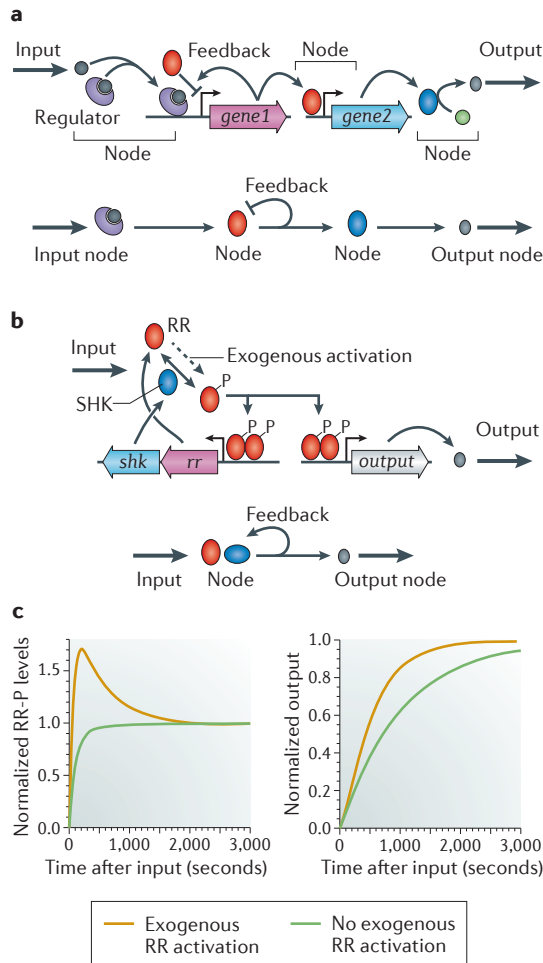


**Figure 1 | Information flow in signalling networks can strongly depend on non-transcriptional details, with important physiological consequences.**

**a** | Components in a transcriptional network. Input signals transfer information via nodes to create a physiological output. The lower schematic is a transcriptional network diagram corresponding to the detailed network in the upper panel. **b** | A typical gene circuit for a two-component system is positively autoregulated by phosphorylated response regulator (RR). The lower schematic is a simplified transcriptional network diagram corresponding to the detailed network in the upper panel. **c** | The system can exhibit feedback-induced overshoot (surge) kinetics if there is a small amount of regulator phosphorylation from an exogenous source in addition to sensor-mediated phosphorylation. In the absence of exogenous phosphorylation, induction is monotonic. Overshoot of regulator phosphorylation speeds the induction of downstream genes (as indicated in the normalized output graph on the right). SHK, sensor histidine kinase.

When exogenous activation of the response regulator occurs alongside signal onset, the level of phosphorylated response regulator overshoots and then settles to a steady state, unlike the monotonic response expected in the absence of exogenous activation<sup>11</sup> (FIG. 1c, left panel). This dynamic is computationally predicted to arise from a negative feedback loop that emerges in the system<sup>11</sup> (see [Supplementary information S1](#) (box)).

Such overshoot kinetics can speed up the induction time of downstream genes (FIG. 1c, right panel) and has profound physiological consequences. In the PhoPQ signalling system of *Salmonella enterica* subsp. *enterica* serovar Typhimurium, overshoot is necessary for virulence<sup>12</sup>. Wild-type bacteria are virulent and kill mice within 10 days. However, removing the overshoot with a feedback-disabling modification to the promoter decreases virulence such that *S. Typhimurium*-injected mice survive indefinitely<sup>12</sup>.

Deducing the relationships between a physiological function, the dynamic response and the underlying molecular mechanisms is crucial if we are to extrapolate from the current handful of laboratory model systems to new, medically important or unculturable bacterial species. Characterization of metabolic, gene-regulatory and protein–protein interaction networks has broadened our understanding of their underlying structures<sup>4</sup>. Nevertheless, a true understanding of the regulatory properties of networks requires that we discover the relationships between mechanistic details and dynamics. These relationships, known as evolutionary design principles<sup>4,13</sup>, are formulated by conducting detailed measurements of dynamics, constructing synthetic gene networks and using mathematical models. Defining the principles that underlie biological regulation will not only facilitate our interpretation of natural networks but also improve our ability to engineer microorganisms to have robust synthetic behaviours with widespread medical and industrial importance. In this Review, we describe the effects of non-transcriptional regulatory processes such as ultrasensitivity, implicit and interacting feedback loops, and spatiotemporal localization of molecules on transcriptional networks, using examples from both natural and engineered bacterial systems.

**The ultrasensitive genetic switch**

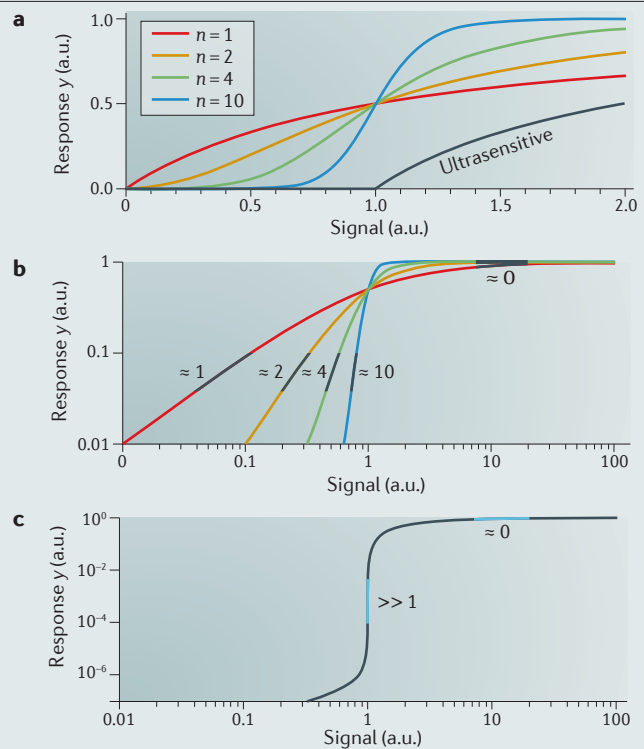
The ability of a biochemical network to respond to an input signal can be characterized by its signal–response curve, or transfer function (BOX 1). For transcriptional networks, such curves show how the expression of downstream genes changes as a function of transcription factor concentration or the reception of activation signals. For transcription factors acting as monomers, the expected dependence resembles Michaelis–Menten kinetics: linear at low signal concentrations and saturated at high signal concentrations<sup>14</sup>. Multimeric transcription factors with cooperativity can produce sigmoidal response curves that are typically captured with Hill kinetics, but the effective cooperativity (that is, the Hill coefficient) is restricted to a low integer number<sup>15</sup>, reflecting the number of subunits present in a complex<sup>16</sup>. By contrast, post-translational signal–response curves are capable of attaining much higher effective cooperativities.

Signal–response systems with high effective cooperativities are usually referred to as ultrasensitive<sup>17</sup>. They are characterized by a sharp transition threshold between the off and on states (BOX 1). The system output will be relatively insensitive to changes in signal either below or above the threshold, remaining unambiguously off or on. Subthreshold signals are absorbed similarly to

## Box 1 | Quantification of signal responses

Signal–response systems are quantified with the mathematical approach of sensitivity analysis. The sensitivity is typically quantified as the derivative, or slope, of the signal–response curve on a log–log scale (see the figure, parts **a** (signal–response curves) and **b,c** (on a log–log scale, with slopes indicated)). With  $n$ th order Hill kinetics, the sensitivity is approximately equal to the Hill coefficient,  $n$ , at low signal and decreases to zero as the response becomes saturated (see the figure, part **b**). In gene regulation, the Hill coefficient is usually limited by small integer values (see the figure, parts **a** and **b**; curves with  $n$  values of 1, 2 or 4). Post-translational interactions can increase the kinetic order to much higher levels (for example,  $n = 10$ ; see the figure, parts **a,b**). In ultrasensitive regimes, low and high signals have smaller sensitivities, whereas an intermediate signal has a very high sensitivity (a slope of 20, 40 or higher), corresponding to a signal–response threshold (see the figure, part **c**).

a.u., arbitrary units.



a small amount of water in a sponge, whereas above-threshold signals are akin to a large quantity of water saturating the sponge and spilling out. Ultrasensitivity to signals in the intermediate range can regulate costly processes that require a decisive response, or programme cells to ignore small or transient signals when the activation of output genes is not advantageous.

Several different molecular mechanisms related to saturation can allow biochemical ultrasensitivity. In the classical covalent-modification mechanism, a protein can be activated and deactivated (for example, by phosphorylation and dephosphorylation) by two competing enzymes near saturation<sup>17</sup>. Ultrasensitivity in covalent-modification systems is important in development, especially in eukaryotes, for creating irreversible lineage commitment<sup>18–20</sup>. Ultrasensitivity also plays a part in bacterial systems — for example, in the chemotactic response of *Escherichia coli*<sup>21</sup> or in the regulation of metabolic enzyme activity<sup>22</sup>. Regulated degradation<sup>23</sup> and stoichiometric sequestration<sup>24</sup> (also referred to as molecular titration; discussed below) can also give rise to ultrasensitivity in bacteria.

#### Ultrasensitivity from stoichiometric sequestration.

Ultrasensitivity can arise from stoichiometric sequestration, in which a protein is kept inactive via strong binding to a specific antagonist<sup>24</sup>. In bacterial transcriptional regulation, alternative RNA polymerase (RNAP)  $\sigma$ -factors are often sequestered by anti- $\sigma$  factors. When the alternative  $\sigma$ -factor is not sequestered, it stimulates RNAP binding to condition-specific promoters. However, if concentrations of  $\sigma$ -factors and anti- $\sigma$  factors

are independently regulated, the transcriptional response will be ultrasensitive to the ratio of their concentration.

For example, the global stress response regulator RNAP factor  $\sigma^E$  in *Mycobacterium tuberculosis* exhibits ultrasensitivity owing to sequestration by the anti- $\sigma$  factor RseA<sup>25</sup>. The fraction of active (free)  $\sigma^E$  changes with the level of total  $\sigma^E$  in an ultrasensitive manner (FIG. 2a). When the concentration of RseA exceeds that of  $\sigma^E$ , most  $\sigma^E$  will be bound by the anti- $\sigma$  factor and there will be little free  $\sigma^E$ . When the concentration of  $\sigma^E$  reaches that of RseA, most  $\sigma^E$  is still sequestered. However, when  $\sigma^E$  abundance surpasses that of RseA, the concentration of free  $\sigma$ -factor sharply increases (FIG. 2a, lower panel). When this alternative  $\sigma$ -factor is abundant, it effectively binds the RNAP core, causing a global shift in gene expression. As a result of the ultrasensitive switch, the anti- $\sigma$  factor RseA buffers the effects of  $\sigma^E$ -mediated changes until a critical stress threshold is reached. A directly analogous situation arises when a constitutively transcribed small RNA (sRNA) (FIG. 2b) binds a target mRNA, preventing translation of the target until the sRNA is saturated, thus determining a precise threshold for protein production<sup>26,27</sup>. In both examples, the ultrasensitivity crucially depends on the strength of the sequestration interaction: with increased binding affinity (a decrease in the dissociation constant), we expect an increase in the effective cooperativity (curves in FIG. 2a,b).

**Ultrasensitivity coupled to positive feedback.** Positive autoregulation can further increase effective cooperativity<sup>28</sup>. The combination of ultrasensitivity and positive

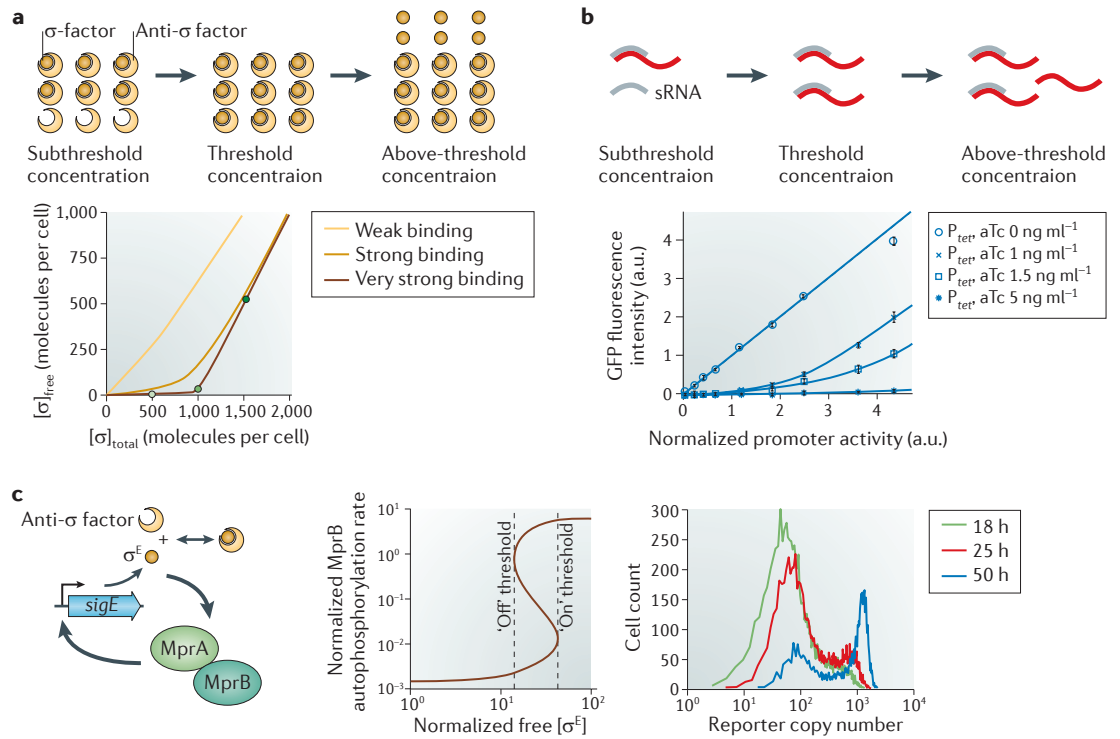


**Figure 2 | Saturation creates an ultrasensitive switch.** **a** | As the total concentration of RNA polymerase  $\sigma$ -factor increases, anti- $\sigma$  factor sequesters it until the critical point is reached, as determined by the concentration of anti- $\sigma$  factor and its affinity for  $\sigma$ -factor. The resulting quantitative effect is a titration curve for free  $\sigma$ -factor (lower panel) that crosses a steep transition into the range where the  $\sigma$ -factor has high concentrations. Comparing the responses for different binding affinities shows that strong binding is necessary for the effect. The dots on the ‘very strong binding’ line indicate the response at a subthreshold  $\sigma$ -factor concentration ( $[\sigma]$ ) (light green), at the threshold  $[\sigma]$  (mid-green) and at an above-threshold  $[\sigma]$  (dark green). **b** | An analogous threshold arises when a small RNA (sRNA) prevents translation of a response mRNA. After the mRNA concentration exceeds a threshold determined by the sRNA concentration (owing to a sufficient level of stress signal), translation of unsequestered mRNA proceeds. Points in the graph (lower panel) represent experimental data from expressing GFP from a gene containing the *crsodB* sRNA recognition sequence in the 5’ untranslated region; sRNA induction conditions were varied by addition of increasing concentrations of anhydrotetracycline (aTc); thus, each line corresponds to a different sRNA concentration. Solid curves are model predictions<sup>26</sup>. **c** | In *Mycobacterium tuberculosis*, RNA polymerase factor  $\sigma^E$  (encoded by *sigE*) upregulates MprAB, a two-component system that regulates stress responses. Positive feedback from the two-component system combined with an ultrasensitive  $\sigma$ -factor–anti- $\sigma$  factor interaction enables a bistable response from MprAB with two ultrasensitive thresholds, as demonstrated by the signal–response curve (middle panel). The right panel shows that simulated single-cell distributions of a reporter for  $\sigma^E$  activity are bimodal, with a growing fraction of cells inducing  $\sigma^E$  after stress initiation. a.u., arbitrary units. Part **b** graph is modified from REF. 26.

feedback can thus create signal–response curves that are characteristic of a bistable switch<sup>28</sup>. Bistable switches have two ultrasensitive thresholds, one for transitioning from the off to the on state, and the other for moving from the on to the off state. These signal–response curves are not only ultrasensitive but also hysteretic — that is, the response of the network to intermediate signal levels differs depending on the history of the cell (whether it was previously exposed to high or low signal concentrations) (FIG. 2c). With two thresholds, the response to signal is similar to a ratchet, turning on or off irreversibly in the absence of a decisive change in signal level. The  $\sigma^E$ –RseA pair in mycobacteria exhibits just such an effect through a feedback loop that operates via the two-component system MprAB (FIG. 2c). Stress-responsive MprA becomes phosphorylated to activate transcription of *sigE* (the gene encoding

$\sigma^E$ ), but with a sudden sharp increase in  $\sigma^E$ , signalling via MprAB is sharply increased, creating a hysteretic switch<sup>25</sup>. Ultrasensitivity resulting from sequestration is essential for attaining bistability<sup>24</sup>. This bistability may enable ‘bet hedging’ during the transition to dormancy in a population of *M. tuberculosis* invading a host<sup>25,29</sup>: noise in the network disperses the signal level around the switch point, causing some subsets of the population to be active and others, inactive for stress response signalling.

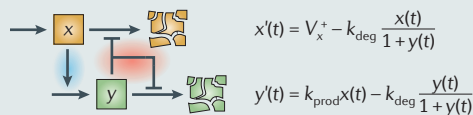
**Single-cell ultrasensitivity.** In the femtolitre volumes of microbial cells, stochastic effects of small numbers of interacting molecules are unavoidable. At the level of cell populations, noise can reduce the apparent effects of ultrasensitivity or bistability<sup>30</sup>. What looks like a discrete switch in a single cell appears to be ‘averaged

Box 2 | Using mathematical tools to identify feedback loops

In a chemical reaction network with established rates of production and degradation for each species, feedback loops can still be difficult to determine by examination. Mathematical tools adapted from chemical engineering can assist in their analysis. One approach, chemical-reaction network theory<sup>98</sup>, exploits topological features of post-translational networks to predict bistability<sup>33</sup>, absolute concentration robustness<sup>99</sup> (for example, using the robustness of regulation by bifunctional two-component systems to predict the expression levels of their proteins<sup>100,101</sup>) and other dynamic properties of networks.

Another approach is to write each molecular subspecies as a system of differential equations and exploit dynamic-systems theory. For example, one can detect implicit feedback loops using a matrix that captures the local sensitivity of all molecular species to each other using partial derivatives, known mathematically as the Jacobian matrix<sup>34</sup>. The Jacobian matrix reveals the extent to which fluxes that produce and degrade one variable depend on others. We may find that variable A depends on variable C, which in turn depends on variable B, which in turn depends on A, so that we have a feedback loop  $A \rightarrow B \rightarrow C \rightarrow A$ . To be sure that all feedback loops are detected, all significant interactions between species (both direct and pleiotropic) should be present in the Jacobian matrix. This task is often challenging owing to subtle physical effects that may need to be determined experimentally.

A simple model for a two-species network in which one species has a ubiquitous inhibitory effect on growth can be diagrammed with each reaction and regulatory interaction, and represented as a set of differential equations, in which  $x$  and  $y$  are the cellular concentrations of each variable;  $V_x^+$ ,  $k_{\text{prod}}$  and  $k_{\text{deg}}$  are kinetic parameters of each reaction; and prime (') denotes the time derivative:



The regulator  $x$  induces production of  $y$ , which inhibits growth-mediated protein degradation (that is, dilution). Here, the Jacobian network is:

$$J = \begin{bmatrix} \frac{\partial x'}{\partial x} & \frac{\partial x'}{\partial y} \\ \frac{\partial y'}{\partial x} & \frac{\partial y'}{\partial y} \end{bmatrix} = \begin{bmatrix} -\frac{k_{\text{deg}}}{1 + y(t)} & \frac{k_{\text{deg}} x(t)}{(1 + y(t))^2} \\ k_{\text{prod}} & -\frac{k_{\text{deg}}}{(1 + y(t))^2} \end{bmatrix} \rightarrow \begin{bmatrix} - & + \\ + & - \end{bmatrix}$$

A mathematical expression for each matrix entry tells us whether each effective interaction has a positive or negative effect on expression of the target. With dependencies within the network determined by the entries in the Jacobian matrix, a circuit diagram of off-diagonal (that is, non-autoregulatory; highlighted in blue) elements simplifies the picture and shows the effects of growth inhibition manifesting as a positive feedback loop:



out' over the population. Ultrasensitivity can therefore often be present, and have important implications for cellular physiology, but be difficult to detect at the population level. Single-cell measurements are therefore a useful experimental tool for detecting ultrasensitive behaviours.

**Implicit feedback loops**

Pleiotropic and post-translational effects can also result in unexpected and indirect interactions between network components. For instance, feedback loops can occur because of subtle or indirect interactions between biochemical reactions<sup>31–34</sup>. These effects can be quantified with appropriate mathematical methods (BOX 2). However, their detection requires detailed experimental data that are often lacking because the important components are not known in advance. A synergistic

combination of mathematical modelling and mechanistic experimental studies can therefore elucidate non-obvious regulatory processes in biological networks.

**Modulation of the growth rate as an implicit feedback loop.** Transcription, gene dosage and protein dilution are affected by cellular growth rates<sup>35</sup>. If the level of an expressed protein has an effect on the growth rate, then production and/or decay rates for that protein also change and an implicit feedback loop arises<sup>35,36</sup>. For example, most proteins in bacteria are stable: the dominant process affecting their concentrations is cell growth and division. At a constant rate of exponential growth, a given protein effectively undergoes first-order degradation. When growth slows down, protein dilution is reduced; during prolonged stress or in stationary phase, induced proteolytic enzymes may degrade proteins<sup>37</sup>, but a stable protein can undergo a sharp increase in concentration during growth arrest. If this protein, or its metabolic product, imposes a burden on growth, a positive feedback loop can arise in relation to protein abundance<sup>35</sup> (FIG. 3).

One predicted consequence of growth-modulated feedback is the bistable phenotype that may be relevant for antibiotic persistence: when the toxin of a toxin–antitoxin system is present at levels above a certain threshold, a slow- or non-growing subset of persister cells develops<sup>38,39</sup> as a result of growth-inhibiting toxin production<sup>35</sup>. During cell division, parental toxin is partitioned into two daughter cells according to a binomial distribution; one daughter cell may receive much more parental toxin than the other (FIG. 3a). Because growth rate decreases as a function of toxin abundance, intermediate levels of toxin production may cause an otherwise identical bacterial population to have two distinct growth rates.

Even if growth rate-linked feedback itself does not result in bistability, it can change critical parameters in a non-bistable network to induce bistability. Such a system was recently constructed in *E. coli* using an autoregulating T7 RNAP<sup>36</sup> (FIG. 3b). In this system, T7 RNAP has a non-cooperative positive feedback effect that, alone, is incapable of inducing bistability. However, the expression of T7 RNAP imposes a metabolic burden on the cell, slowing cell growth and resulting in an implicit positive feedback loop. Together, the two loops create a bistable switch. As with the bistable  $\sigma^E$ –MprAB system described above, in the population as a whole, noise disperses the gene expression level to the two stable states simultaneously. This can be observed as two distinct subpopulations of cells with low and high levels of expression for a T7 RNAP reporter (FIG. 3b).

**Implicit feedback arising from enzymatic interactions.**

In addition to the implicit feedback that can result from growth rate-dependent pleiotropic effects, this type of feedback can arise from the modulation of catalytic reactions by substrates, products or cofactors<sup>33</sup>. For example, substrate inhibition<sup>40</sup> can lead to a non-monotonic dose response in enzyme catalysis, resulting in a feedback loop that allows bistability: more substrate inhibits the conversion of substrate to product, resulting in more

**Bistable switch**

A system in which there are two stable steady states under the same conditions, as reflected in the signal–response curve. Which state the system adopts in practice depends on the initial conditions and noise.

**Bet hedging**

An evolved phenotype that employs heterogeneity to ensure that distinct subsets of a cellular population are adapted to different outcomes of an unpredictable future environment.

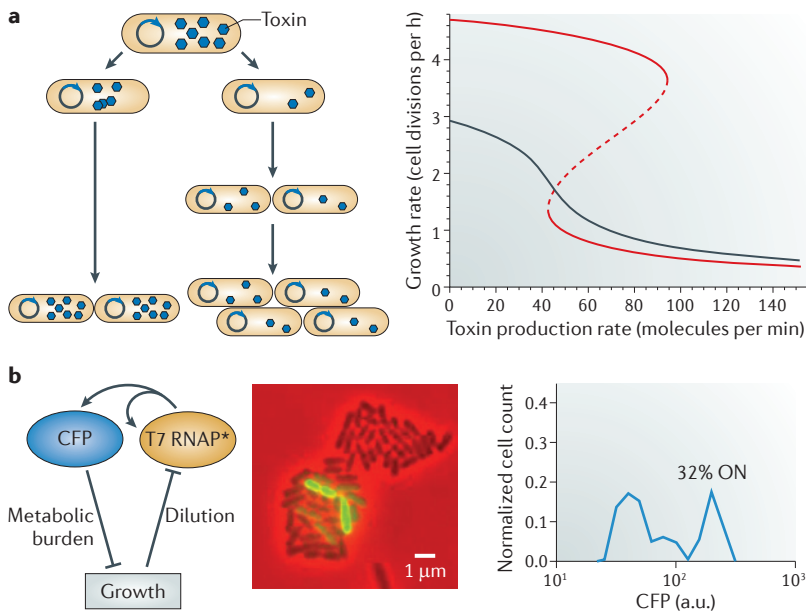


**Figure 3 | Modulation of growth rate can create an implicit feedback loop with two resulting subpopulations of bacteria. a** | A toxin expressed from a plasmid is unequally partitioned into two daughter cells. With a higher toxin concentration, growth is slower, allowing more toxin to build up (as the cell is still expressing the toxin from the plasmid). The result of the feedback loop is a nonlinear relationship between the strength of the toxin promoter and the growth rate of the cell. A mathematical model (right panel) predicts two resulting subpopulations of cells growing at different rates under some conditions (red curve; the dashed portion represents an unstable intermediate steady state), and unimodal populations with a nonlinear toxin response under other conditions (black curve)<sup>35</sup>. **b** | A synthetic system in *Escherichia coli* with autoregulating T7 RNA polymerase (RNAP) that also upregulates a fluorescent protein (CFP) as a readout. A second, implicit feedback loop arises from the metabolic burden of gene expression. Microcolonies of the synthetic strain exhibit bimodal fluorescence (visible as both dark and green cells; middle panel) as a result of bistability<sup>36</sup>, as shown by the model (right panel). a.u., arbitrary units. Part **b** is reproduced, with permission, from REF. 36 © (2009) Macmillan Publishers Ltd. All rights reserved.

**Noise**

Variability in signals and responses from cell to cell that arises either intrinsically, from the nature of the physicochemical processes, or from extrinsic variability such as randomness in ribosome inheritance.

**Jacobian matrix**

A matrix for which the entries quantitate the sensitivity of each variable (often corresponding to chemical species) to each other variable.

**Implicit feedback loop**

A feedback loop for which its existence is not obvious, but which emerges from non-transcriptional interactions.

substrate<sup>41</sup>. An implicit positive feedback loop can also be induced by interacting proteins forming a long-lived, catalytically inactive ‘dead-end’ complex<sup>31,32,42</sup>. For example, in the partner-switching network that controls the activity of RNAP factor  $\sigma^F$  in *Bacillus subtilis*<sup>31,32</sup>, SpoIIAB is an anti- $\sigma$  factor that binds and inhibits  $\sigma^F$  unless it is sequestered by unphosphorylated SpoIIAA. The level of unphosphorylated SpoIIAA is regulated by the kinase activity of SpoIIAB and phosphatase activity of SpoIIE. SpoIIAB can bind ATP or ADP, and formation of the ADP-associated SpoIIAB–SpoIIAA complex results in the slow conversion of SpoIIAB–ADP to SpoIIAB–ATP (as nucleotide exchange is not possible before the complex dissociates). The complex is self-enhancing because it sequesters SpoIIAB from kinase activity, thus increasing the fraction of unphosphorylated SpoIIAA that is available to bind to ADP-associated SpoIIAB. This feedback loop irreversibly commits the pre-spore compartment to sporulation.

**Untangling coupled feedback loops**

Simple model systems of single feedback loops have provided valuable insight into the dynamics of biological

networks. However, natural networks often contain a complex mesh of gene-regulatory and biochemical interactions<sup>43</sup>. Even after the implicit feedback loops, ultrasensitive switches and other nonlinearities have been identified for a network, coupled feedback loops and biochemical interactions can add another level of sophistication to physiological responses. The resulting dynamics may depend on mechanistic details: extrinsic inputs, transcription rates and binding constants. A single sufficiently complex network architecture can perform many different dynamic functions; this multifunctionality has been linked to evolvability<sup>6</sup> and may thus result in selection for network complexity. Complex network architectures can also arise from evolutionary drift with no particular selective pressure<sup>44,45</sup>.

How do we determine the physiological relevance of a complex network architecture? One approach is to use perturbations or deletions of network components to systematically characterize the interconnections. For instance, one can break a feedback loop and compare the dynamic performance of this modified network to that of the intact network, or use steady-state properties to infer feedback effects. Experimentally, transcriptional feedback can be broken by replacing a feedback-modulated promoter with a constitutive or inducible promoter<sup>46</sup> or by deleting genes in the network. Similarly, networks can be rewired *in silico* using mathematical models (see Supplementary information S1 (box))<sup>11,47</sup>. Measurements of the open-loop gain — that is, the response of a network output to changes in the level of inducer — can then allow determination of the effect of feedback (taking into account both positive and negative interactions). For some networks, characterization of the open-loop response can reveal whether the network can be bistable (see Supplementary information S1 (box)). However, the deletion of genes risks complicating the fine-tuned control of the system and moving away from the steady state of the intact system.

**Systematic experimental perturbation of feedback.**

Recent studies of the glutamate-dependent acid response, acid resistance system 2 (AR2), in *E. coli*<sup>48,49</sup> used a combination of feedback loop deletions and systematic network perturbations to decrypt the elements responsible for this complex dynamic response. When an *E. coli* culture is exposed to low pH, the acid-responsive two-component system EvgAS becomes activated. One of the operons in the regulon of phosphorylated EvgA is *safAydeO*; sensor-associating factor A (SafA; also known as B1500) forms a negative feedback loop with the two-component system PhoPQ, whereas YdeO upregulates the glutamic acid decarboxylase operons *gadE* and *gadBC* directly and indirectly, respectively (FIG. 4a,b). This subnetwork induces a fast immediate response with an overshoot, as measured by promoter–luciferase reporter gene fusions<sup>49</sup> (FIG. 4c, the first 60 minutes). Phosphorylated PhoP, the result of the SafA interaction with the PhoPQ system, not only represses *safAydeO* but also induces transcription of *iraM*<sup>48</sup> — encoding an anti-adaptor that inhibits the RssB-mediated proteolysis of RNAP factor  $\sigma^S$  (encoded by *rpoS*) — thereby activating  $\sigma^S$  when the stress is

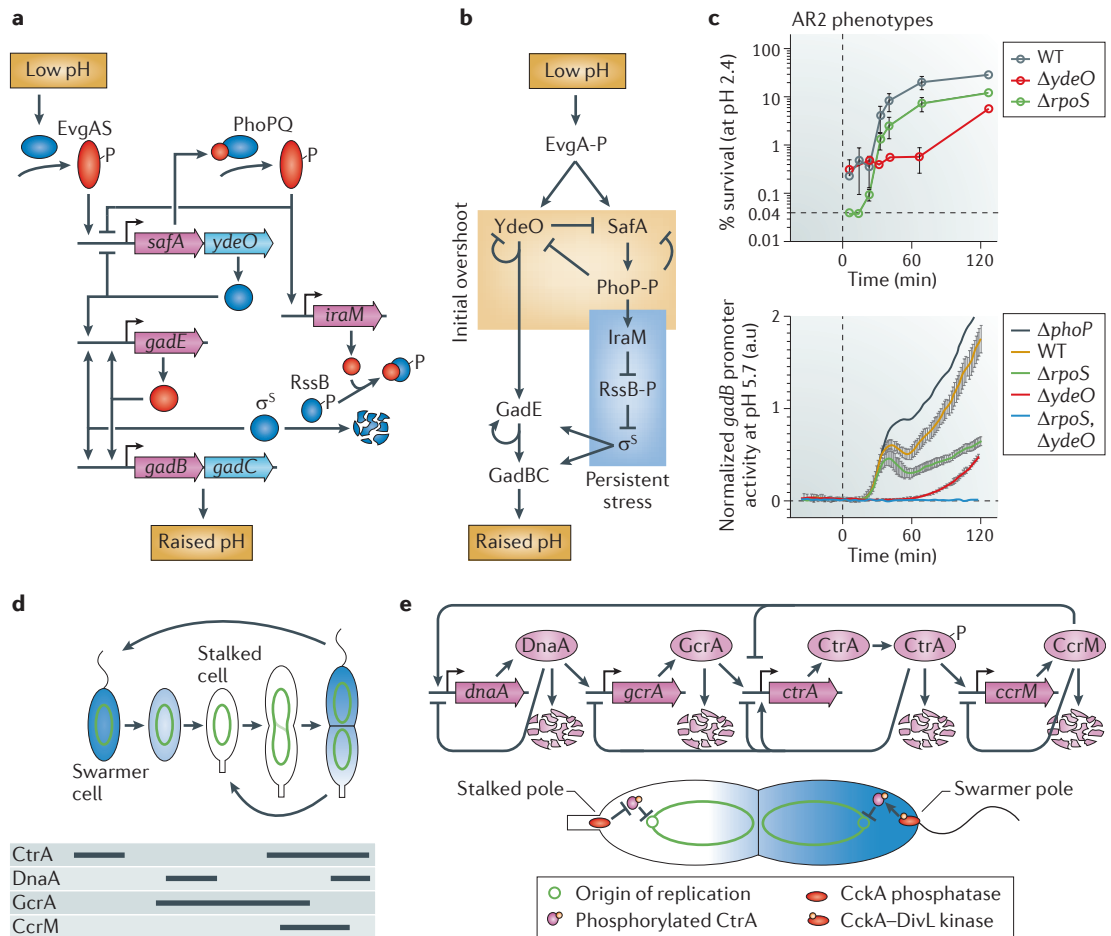


**Figure 4 | Complex feedback architecture with non-transcriptional interactions enables complex dynamic responses.** **a** | The *Escherichia coli* glutamate-dependent acid response system, acid resistance system 2 (AR2), is a complex network with interleaved transcriptional–post-translational interactions that responds to acid stress on two timescales: an initial low pH feeding into the EvgAS two-component system, and upregulation of alternative RNA polymerase factor  $\sigma^S$  in response to persistent stress<sup>48,49</sup>. **b** | A circuit diagram reveals a negative feedback architecture for early responses in the AR2 system (pre-60 minutes) and a coherent feedforward loop under persistent stress. **c** | High-temporal-resolution measurements of promoter kinetics in the AR2 system show two response phases: a fast, overshooting response from the initial, negative feedback loop and a persistent high-expression response imparted by the  $\sigma^S$ –Gad feedforward loop<sup>49</sup>. Systematic deletion mutants that have lost various dynamic characteristics show the role of each feedback loop in the emergent AR2 biphasic system response. **d** | The *Caulobacter crescentus* cell cycle has evolved to deterministically produce daughter cells with two different developmental phenotypes: a transient swarming cell type and a mature stalked cell type. Each cell cycle stage has a characteristic expression of core genetic-circuitry components, as indicated in the lower panel (black lines show expression during that stage). **e** | The core genetic programme of *C. crescentus* cell division is a feedback circuit that depends on regulated degradation to attain oscillatory behaviour. A spatial gradient of cell cycle transcription regulator (CtrA) phosphorylation, mediated by the polar localization of cell cycle histidine kinase (CckA) kinase and phosphatase activities, suppresses chromosome replication in the swarmer pole (where CckA acts as a kinase) but not in the stalked pole (where CckA acts as a phosphatase). Blue shading represents the gradient of phosphorylated-CtrA concentration. a.u., arbitrary units; Gad, glutamic acid decarboxylase.

**Toxin–antitoxin system**

A small gene network that typically includes one gene encoding a toxin and another encoding a neutralizing antitoxin.

**Coupled feedback loops**

Multiple feedback loops that interact in some way, such as being nested or resulting from a single regulatory event that modulates multiple transcriptionally coupled genes.

**Dynamic performance**

The characteristics of a response to a signal over time.

**Biphasic**

Of a response: composed of two distinct, characteristic types of dynamics that are separated in time, such as an initial transient phase and a long-term persistent phase.

persistent and ultimately upregulating the *gadE* and *gadBC* operons (FIG. 4c, after 60 minutes). In one study, wild-type responses were compared with open-loop dynamics created by deletion of *phoP*, *ydeO* and *rpoS*<sup>49</sup> (FIG. 4c). Using these results, and accounting for non-transcriptional interactions, the underlying circuit diagram was constructed and gave clues to the function of the acid response network. This network employs a biphasic dynamic with a fast initial response and a persistent, high-expression phase for when the stress is ongoing.

The first phase is mediated by negative feedback, which has long been known to speed up induction dynamics<sup>50</sup>. The second phase involves a feedforward loop to the output stress response genes, a type of regulation that is known to cause signal delays in a sign-sensitive manner (that is, according to whether the feedback is positive or negative; in this case, the deactivation of gene expression, rather than its activation, is delayed because the *gabBC* promoter acts as an OR gate, thus requiring both signals (GadE and  $\sigma^S$ ) to be lost to stop gene expression)<sup>5,8</sup>.

Such an interleaved architecture makes initial responses fast and decisive, whereas persistent responses maintain high levels of expression for long time periods. The result of this complex network architecture is more effective survival in acidic environments<sup>49</sup> (FIG. 4c, upper panel).

**Feedback architectures for complex dynamic responses.** Mounting evidence suggests that the biphasic response is a general bacterial survival strategy that emerges from complex feedback architecture. An important example is the stringent response, during which amino acid starvation is sensed during translation by RelA, a ribosome-associated protein that produces guanosine tetraphosphate (ppGpp) as an activator of amino acid biosynthesis. Biosynthesis of amino acids relieves starvation, acting as a negative feedback loop that prevents induction of the generalized stress response<sup>51</sup>. However, if biosynthesis is unsuccessful, sufficient ppGpp accumulates to induce the  $\sigma^S$ -mediated stress response and prepare the cell for long-term survival<sup>51</sup>. Similarly, autoregulated two-component systems in the presence of an exogenous source of response regulator phosphorylation are predicted to exhibit either negative feedback (for initial induction with fast responses) or positive feedback (for persistent stress responses with high expression), depending on signal strength<sup>11</sup> (see Supplementary information S1 (box)). Negative feedback is associated with overshoot kinetics (FIG. 1), whereas positive feedback confers a robustness to transient signal interruptions<sup>3,4,52</sup>.

The biphasic dynamics arising from a complex feedback architecture can also manifest as two subsets of a bacterial population simultaneously exhibiting different phenotypes. There are several known examples of such systems with coupled positive feedback loops. In *B. subtilis*, positive feedback in several steps of the Spo0A sporulation phosphorelay generates noise, increasing the variability of phosphorylated-Spo0A levels in the population<sup>53</sup>. As a result, a fraction of the cells exceed the downstream threshold for sporulation entry, and both vegetative and sporulating subpopulations coexist, in a bet-hedging strategy. The Spo0A system is an integrated part of a larger network that appears to ratiometrically integrate quorum sensing signals along with stress signals<sup>54</sup> and that interacts with competence regulation<sup>55</sup>, showing that population structure and cell-to-cell communication can become a part of the decision circuit. Multiple positive feedback loops also occur in Gram-negative bacteria: in *Salmonella* spp., the type III secretion system encoded by the *Salmonella* pathogenicity island 1 (SPI-1) is controlled by a coupled set of transcription factors that positively regulate one another to both impose a discrete threshold on SPI-1 gene expression and increase expression levels when induced<sup>56</sup>.

Coupled negative feedback loops have important physiological consequences as well. Their effects typically depend on details such as delays between the signal and response, caused by signal processing steps such as transcription, translation, protein folding and protein multimerization. Whereas negative feedback without a delay improves the response times<sup>50</sup> and reduces noise<sup>57</sup>,

persistent oscillations and increased noise can arise with delays in the response<sup>58,59</sup> or with consumption of end products in metabolic pathways<sup>58,60</sup>. Multiple negative feedback loops stabilize the system and improve homeostasis by eliminating these effects<sup>61</sup>.

**Non-transcriptional cell cycle control.** The Gram-negative bacterium *Caulobacter crescentus* is a model bacterium in which coupled networks of post-translational spatiotemporal control regulate the cell cycle<sup>62</sup>. Each division in *C. crescentus* is a finely orchestrated process that results in the simultaneous production of two distinct daughter cells: a swarmer cell and a stalked cell (FIG. 4d). The swarmer cell undergoes a brief motile stage before maturing to the stalked phenotype, attaching to a surface and resuming asymmetrical cell division. Unlike the two populations that coexist in bacteria which have adopted a bet-hedging strategy, such as *B. subtilis*, these two *C. crescentus* cell types are maintained deterministically: every mother cell cycle produces one stalked and one swarmer daughter.

The core regulatory circuit consists of four genes expressed at specific points during the cell cycle (FIG. 4d). Each gene product regulates multiple downstream cell cycle-specific genes. In one model, the four gene products form a positive feedback loop. Within the larger positive loop, the phosphorylated form of cell cycle transcription regulator (CtrA), the master regulator, is at the centre of two negative loops, one with GcrA and one with the methylase CcrM (also known as CcrMI) (FIG. 4e). Repeated expression of the same genes in the same order, over many consecutive cell cycles, depends on fast, regulated turnover of the protein products via proteolytic degradation<sup>63</sup> (FIG. 4e). For stable proteins, signal loss depends on dilution via cell growth and division, a much slower process than is needed for brief expression during a short fraction of a cell cycle. So, with induced degradation of each gene product, the core cell cycle genes are expressed in distinct pulses for discrete periods, forming an oscillator<sup>63</sup>. Such oscillatory dynamics prevent competition between signals for different stages in the cell cycle.

The asymmetric character of *C. crescentus* cell division depends on both a spatial signalling gradient in the master regulator CtrA and maintenance of the chromosome in a polarized physical orientation<sup>64</sup>, with the origin of replication at the stalked pole before replication initiation. The crucial parameter is the amount of phosphorylated CtrA. The bifunctional protein cell cycle histidine kinase (CckA), which can act as a kinase and a phosphatase, modulates CtrA phosphorylation and is under feedback control by phosphorylated CtrA itself<sup>65,66</sup>. When CtrA is phosphorylated, CckA is mainly localized to the polar regions of the pre-divisional cell. The CckA at the stalked pole has CtrA phosphatase activity, whereas the CckA at the swarmer pole exhibits kinase activity owing to its interaction with DivL<sup>67</sup>. A recent study coupled mathematical analysis with experimental, spatially-resolved measurements of CtrA-regulated initiation of DNA replication<sup>67</sup> to elegantly demonstrate the phosphorylatory control that allows replicative asymmetry in these cells<sup>67</sup>. Nevertheless,

#### Robustness

Insensitivity of a dynamic performance to small parameter perturbations that would arise from intrinsic or extrinsic noise, slight environmental variations, and so on (for the purposes of this Review; the term has many subtly different meanings in systems biology).

#### Oscillator

A network architecture that results in periodic oscillations of an output.

the gradient in total CtrA probably contributes to the cell cycle: perturbations in CtrA proteolysis and CckA activity buffer each other<sup>62</sup>. This type of partial redundancy of non-transcriptional processes ensures that the cell cycle proceeds robustly in the presence of noise. The complexity of the *C. crescentus* cell cycle control network, combining transcriptional and non-transcriptional interactions, may therefore have evolved in response to selective pressure for a robust phenotype.

Spatial gradients and oscillatory dynamics of cell cycle regulation also appear in other bacterial species. CtrA-modulated cell cycle regulation is conserved in alphaproteobacteria<sup>68</sup>. Studies have shown that stalked cells undergo ageing and that decreasing reproduction is associated with a specific stalked-cell pole<sup>69</sup>, an effect that has been generalized to the morphologically symmetrical gammaproteobacterium *E. coli*<sup>70</sup>.

### Mechanistic synthetic biology

Non-transcriptional nonlinearities, implicit interactions and overall complexity underscore the challenges of studying natural networks. Improved knowledge of, and control over, network architectures is essential for a better understanding of their function. These issues have driven researchers to construct synthetic biological networks that function as tractable laboratory models and allow a more thorough understanding of phenotype at the level of genotype<sup>71</sup>.

### Challenges in constructing synthetic gene networks.

In early synthetic biological networks, signals were often encoded as the number of protein transcription factors in a cell<sup>72–76</sup>. In this type of network, the precision of signal transmission is limited by the noise in gene expression. Random production and degradation of mRNAs<sup>77</sup> and proteins<sup>78</sup>, transmitted fluctuations from other molecules in the network<sup>78,79</sup> and variations in global factors such as polymerases and ribosomes<sup>80</sup> reduce the precision with which a given protein can be expressed. Indeed, the standard deviation in protein abundance across a population of cells is often 10–50% of the mean<sup>81</sup>. Because many transcription factors bind strongly to their promoters, small changes in transcription factor concentration can substantially change promoter activity. In such circumstances, fluctuations can lead to signal degradation in an individual cell and dramatic differences in the behaviours of networks in neighbouring cells. These fluctuations can, in turn, result in a breakdown in the function of the synthetic network<sup>75</sup>.

Signal matching is another difficulty that arises in the construction of synthetic gene networks. The range of output signal produced by a given node can be improperly matched with the range of signal to which another node can respond. For example, if two promoters are connected in series, leaky expression of a transcription factor from the first promoter may be sufficient to strongly activate or repress the second<sup>72,76</sup>. In such a case, the downstream promoter effectively becomes ‘deaf’ to information coming from the upstream promoter, and the network can lose its dynamic range of response or become non-functional<sup>72,76,82</sup> (FIG. 5a).

**Control of translation rate.** Various methods have been used to match signal strengths in synthetic gene networks<sup>73,76,82–84</sup>, with modification of translation initiation rates being a particularly successful approach (FIG. 5a). For a given protein, the mRNA sequence surrounding the start codon of the encoding transcript regulates total abundance in the cell. Among other parameters, the distance of the ribosome-binding site (RBS) from the start codon and the degree of mRNA base pairing with 16S ribosomal RNA control the rate of translation and, thereby, protein concentration. RBS swapping<sup>73</sup> and directed evolution<sup>82</sup> have been used to tune the abundances of signal-carrying proteins in transcriptional networks. Recently, thermodynamic models that allow the *de novo* design of RBS sequences with desired translation rates have been developed<sup>84,85</sup>. New DNA assembly methods make it possible to place a synthetic RBS sequence in front of any ORF without leaving scars from restriction enzyme sites<sup>86</sup>. This type of seamless sequence replacement is important when cloning RBSs, as their activity is strongly dependent on adjacent nucleotide sequences<sup>84</sup>.

**Robust oscillations via post-translational control.** One goal of synthetic biology is to engineer networks that are capable of generating robust, dynamic cellular behaviours. A particularly challenging behaviour is that of persistent oscillations. The first attempt to construct an oscillator, known as the repressilator, used three transcriptional repressors organized in a ring topology<sup>75</sup>. If any repressor achieved a high concentration, it would repress the next member of the network, so the third repressor would increase in abundance, subsequently repressing the first. Although this topology gave rise to oscillations, they were short lived and unstable, unlike the robust natural oscillations that occur in organisms such as *C. crescentus*. Because signal is carried as transcription factor abundance, noise in gene expression is thought to compromise the performance of the repressilator<sup>75,81</sup>.

Recently, it was demonstrated that non-transcriptional effects can have an important role in the performance of oscillatory transcriptional networks<sup>87,88</sup>. In one engineered network, the arabinose-dependent transcription factor AraC was engineered to activate transcription of its encoding gene and of the lactose (*lac*) operon repressor gene (*lacI*)<sup>87</sup>. In this way, when arabinose was present, both AraC and LacI rose in abundance. After accumulating to a considerable level, LacI dominantly repressed transcription of *araC*. Both transcription factors were tagged for proteolytic degradation, causing their abundances to decrease rapidly when AraC was not produced. A mathematical model of the network suggests that delays in the LacI-mediated negative feedback step, arising from transcription, translation, protein folding, protein multimerization and DNA binding, are crucial for robust oscillations. Indeed, the longer the negative feedback delay, the more robust the oscillations are to changes in network parameters<sup>87</sup>. Although the general properties of negative feedback-driven oscillatory networks have long been known, the construction of this synthetic network highlighted the impact that these more subtle processes can have on the performance of gene networks.

#### Signal matching

Adjusting the amount of signal produced by an upstream node so that it is within the range to which a downstream node is responsive (unsaturated).

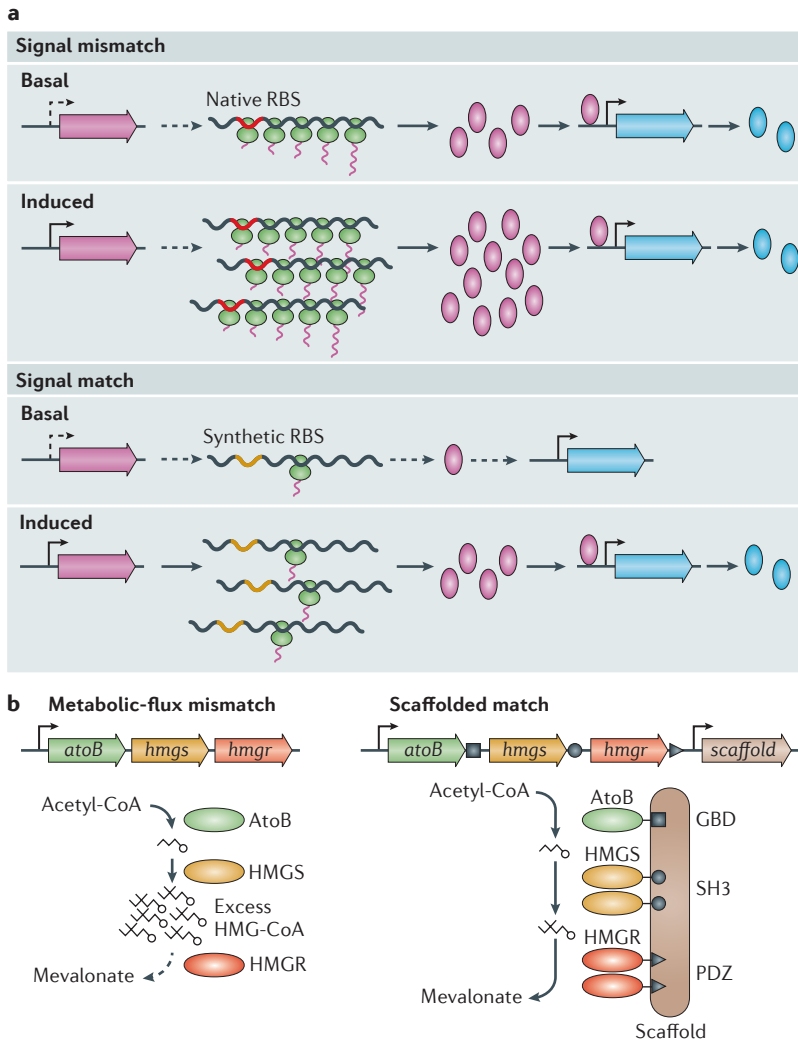


**Figure 5 | Engineering non-transcriptional processes for synthetic biology.** **a** | Leaky transcription can produce sufficient signal to flood downstream nodes. Signal matching can be achieved by engineering the ribosome-binding site (RBS) to prevent low-level transcription from causing extraneous downstream signalling<sup>84</sup>. **b** | A similar mismatch occurs in a synthetic metabolic pathway for mevalonate production. When the synthetic enzymes are present as individual proteins (left panel), the undesired intermediate hydroxymethylglutaryl-CoA (HMG-CoA) builds up, as HMG-CoA reductase (HMGR) cannot keep up with the flux in the system. By placing the enzymes in the pathway onto a physical scaffold (right panel), containing various domains (GBD, SH3 and PDZ) to which the pathway enzymes are engineered to bind, the relative numbers of the enzymes in the scaffold can be manipulated, and the short distances between the enzymes ensures a rapid flux of the intermediates through the system and prevents the accumulation of the product, mevalonate<sup>90,91</sup>. HMGS, HMG-CoA synthase.

In a follow-up study, the performance of engineered oscillators was further improved by employing a cell membrane-diffusible acyl-homoserine lactone (AHL) signalling molecule from the quorum sensing system of *Vibrio fischeri*<sup>88</sup>. In this network, AHL activates its own production and that of *N*-acyl-homoserine lactonase (AiiA), which degrades it. AHL is also a ligand for the transcription factor LuxR, acting much like arabinose in the previously described oscillator. In this enhanced system, the concentration of AHL is proportional to the abundance of the enzymes that produce and degrade

it, and it probably serves to average out the noise in the expression of these proteins. The fact that AHL is membrane diffusible also drives neighbouring cells to occupy the same signalling state at the same time. Beyond driving the bacteria to oscillate in synchrony, this type of population averaging also improves the robustness of the network in any individual cell. Any cell that begins to drift from the synchronized signal range is drawn back into the oscillatory regime by the influence of neighbouring cells.

**Physical colocalization improves signal flow.** Signal flow through a network can also be regulated by controlling physical interactions between signalling nodes<sup>89</sup>. It was recently demonstrated that metabolite flux through a carbon-catabolic pathway can be dramatically improved by scaffolding otherwise freely diffusing metabolic enzymes into a multiprotein complex<sup>90,91</sup> (FIG. 5b). Two *Saccharomyces cerevisiae* enzymes were introduced into *E. coli* to generate mevalonate, a precursor to the antimalarial compound artemisinin<sup>92</sup>. It was found that a major limiting factor for this pathway was the proper matching of the three nodes. In the first design, the upstream enzymes in the pathway (AtoB and hydroxymethylglutaryl-CoA (HMG) synthase (HMGS)) generated a large amount of metabolic product, and a comparatively slow third enzyme (HMG-CoA reductase (HMGR)) produced a bottleneck. Overexpression of HMGR failed to substantially alleviate the problem owing to the growth burden of its production in *E. coli*. The problem was solved by tethering different numbers of the three enzymes together on a synthetic protein scaffold constructed from a translational fusion of three mammalian protein-protein interaction domains (SH3, PDZ and GBD)<sup>91</sup>. Scaffolding two HMGS and two HMGR molecules to a single AtoB enzyme resulted in a nearly 80-fold increase in yield over the unscaffolded system, but other stoichiometries were less efficient. The large increase in yield occurred at low absolute enzyme abundance, decreasing the overall metabolic burden imposed on the host cell.

Improvements arising from scaffolding are probably due to higher local concentrations of pathway intermediates, reduction of the accumulation of toxic intermediates throughout the cell and proper input-output matching of nodes with different enzymatic rates. From a design perspective, matching the input and output by scaffolding is analogous to tuning RBSs for diffusible signal carriers: the total strength of a given node can be raised or lowered by engineering the efficiency of the node.

**New inspiration for the biological-network designer.** Not surprisingly, physical interactions underlie signal processing in natural systems as well. One remarkable example is the stressosome, a 1.8 MDa *B. subtilis* protein complex that contains a symmetrical core structure reminiscent of a viral capsid, decorated with an array of outwards-facing sensor proteins. The sensors seem to detect a variety of stresses, such as ultraviolet light, pH fluctuations and ethanol<sup>93</sup>. Each sensor is oriented to transmit a signal from the outside inwards as a phosphorylation event within the stressosome core. Phosphorylation results in the release of an enzyme that activates the alternative RNAP factor

$\sigma^B$  (REF. 94). Most early synthetic biological networks were inspired by the circuits of electrical engineering. Systems such as the stressosome, however, demonstrate that biology can process signals using approaches that a mechanical engineer might envision as well. Although we are far from being able to design macromolecular structures this sophisticated, we would be well served by taking inspiration from biological networks in all of their varied forms.

### Concluding remarks

The rise of genomics and systems biology has greatly enhanced our understanding of the molecular organization of life, and in particular of microbial life. Recent studies, highlighted here, demonstrate that broad systems-level analysis must be deepened with consideration of molecular mechanisms and non-transcriptional effects. Mechanistic details such as growth rates, spatial gradients, implicit feedback loops and other characteristics can alter the properties of gene expression programmes. The ability to deeply understand life, and to engineer it for useful purposes, requires these effects to be taken into account.

The mechanistic approach to understanding biological networks has important implications for the uses of mathematical models and their relation to experiments. The theoretical foundation of biology is not the networks themselves, but rather their underlying physics. Relevant models, both conceptual and mathematical, must reflect the chemical physics of matter: atoms and molecules interacting in space. It is from these interactions that sophisticated gene expression programmes arise. Physics has constrained evolution and must be remembered when building a model, performing an experiment or designing a synthetic network.

The importance of mechanism — both evolutionary and physical — underscores the importance of quantitative experiments. Microbiologists are moving towards an experimental approach that is guided by, and guiding, theory. Such complementary approaches are necessary for the next generation of life sciences. The quantitative effects of ultrasensitivity, implicit and complex feedback networks, and spatiotemporal organization of genetic programmes, as covered in this Review, exemplify the importance of non-transcriptional processes. Many other quantitative processes and characteristics outside the scope of this Review are known to exist, including transcriptional coupling<sup>95</sup>, DNA-mediated interactions such as promoter cooperativity<sup>96</sup>, and multicellular effects<sup>97</sup>; other examples probably await discovery.

Synthetic-network design has benefited from the combined use of transcriptional and non-transcriptional interactions. The fact that synthetic networks are subject to the same mechanistic rigors and challenges as a natural system makes them an important scientific tool: they enable the comprehensive quantitative experiments that are needed to deepen our biological understanding. Indeed, characterization of these networks in living cells has revealed subtle physical effects, the impacts of which were not widely appreciated a priori. Feedback between synthetic and systems biology will pave the way towards the important medical and industrial applications that will no doubt arise from our deepened understanding of biological networks. The complementary approach of synthetic-network construction alongside quantitative network analysis stands to contribute, perhaps more than any other single approach, to our understanding of the organizing principles of biology.

- Cosentino Lagomarsino, M., Jona, P., Bassetti, B. & Isambert, H. Hierarchy and feedback in the evolution of the *Escherichia coli* transcription network. *Proc. Natl Acad. Sci. USA* **104**, 5516–5520 (2007).
- Balázsi, G., Heath, A. P., Shi, L. & Gennaro, M. L. The temporal response of the *Mycobacterium tuberculosis* gene regulatory network during growth arrest. *Mol. Syst. Biol.* **4**, 225 (2008).
- Wall, M. E., Hlavacek, W. S. & Savageau, M. A. Design of gene circuits: lessons from bacteria. *Nature Rev. Genet.* **5**, 34–42 (2004).
- Alon, U. *An Introduction to Systems Biology: Design Principles of Biological Circuits* (Chapman and Hall/CRC, 2006).
- Mangan, S. & Alon, U. Structure and function of the feed-forward loop network motif. *Proc. Natl Acad. Sci. USA* **100**, 11980–11985 (2003).
- Voigt, C. A., Wolf, D. M. & Arkin, A. P. The *Bacillus subtilis* SIN operon: an evolvable network motif. *Genetics* **169**, 1187–1202 (2005).
- Prill, R. J., Iglesias, P. A. & Levchenko, A. Dynamic properties of network motifs contribute to biological network organization. *PLoS Biol.* **3**, e343 (2005).
- Wall, M. E., Dunlop, M. J. & Hlavacek, W. S. Multiple functions of a feed-forward-loop gene circuit. *J. Mol. Biol.* **349**, 501–514 (2005).
- Stock, A. M., Robinson, V. L. & Goudreau, P. N. Two-component signal transduction. *Annu. Rev. Biochem.* **69**, 183–215 (2000).
- Martínez-Antonio, A., Janga, S. C. & Thieffry, D. Functional organisation of *Escherichia coli* transcriptional regulatory network. *J. Mol. Biol.* **381**, 238–247 (2008).
- Ray, J. C. J. & Igoshin, O. A. Adaptable functionality of transcriptional feedback in bacterial two-component systems. *PLoS Comput. Biol.* **6**, e1000676 (2010).
- Shin, D., Lee, E.-J., Huang, H. & Groisman, E. A positive feedback loop promotes transcription surge that jump-starts *Salmonella* virulence circuit. *Science* **314**, 1607–1609 (2006).
- This study demonstrates the physiological importance of network dynamics for a virulent microorganism.**
- Savageau, M. A. Design principles for elementary gene circuits: elements, methods, and examples. *Chaos* **11**, 142–159 (2001).
- Chen, W. W., Niepel, M. & Sorger, P. K. Classic and contemporary approaches to modeling biochemical reactions. *Genes Dev.* **24**, 1861–1875 (2010).
- Hlavacek, W. S. & Savageau, M. A. Subunit structure of regulator proteins influences the design of gene circuitry: analysis of perfectly coupled and completely uncoupled circuits. *J. Mol. Biol.* **248**, 739–755 (1995).
- Perutz, M. F. Mechanisms of cooperativity and allosteric regulation in proteins. *Q. Rev. Biophys.* **22**, 139–237 (1989).
- Goldbeter, A. & Koshland, D. E. An amplified sensitivity arising from covalent modification in biological systems. *Proc. Natl Acad. Sci. USA* **78**, 6840–6844 (1981).
- Kim, S. Y. & Ferrell, J. E. Substrate competition as a source of ultrasensitivity in the inactivation of Wee1. *Cell* **128**, 1133–1145 (2007).
- Palani, S. & Sarkar, C. A. Positive receptor feedback during lineage commitment can generate ultrasensitivity to ligand and confer robustness to a bistable switch. *Biophys. J.* **95**, 1575–1589 (2008).
- Wang, L. *et al.* Bistable switches control memory and plasticity in cellular differentiation. *Proc. Natl Acad. Sci. USA* **106**, 6638–6643 (2009).
- Cluzel, P., Surette, M. & Leibler, S. An ultrasensitive bacterial motor revealed by monitoring signaling proteins in single cells. *Science* **287**, 1652–1655 (2000).
- LaPorte, D. C. & Koshland, D. E. Phosphorylation of isocitrate dehydrogenase as a demonstration of enhanced sensitivity in covalent regulation. *Nature* **305**, 286–290 (1983).
- Buchler, N. E., Gerland, U. & Hwa, T. Nonlinear protein degradation and the function of genetic circuits. *Proc. Natl Acad. Sci. USA* **102**, 9559–9564 (2005).
- Buchler, N. E. & Louis, M. Molecular titration and ultrasensitivity in regulatory networks. *J. Mol. Biol.* **384**, 1106–1119 (2008).
- Tiwari, A., Balázsi, G., Gennaro, M. L. & Igoshin, O. A. The interplay of multiple feedback loops with post-translational kinetics results in bistability of mycobacterial stress response. *Phys. Biol.* **7**, 036005 (2010).
- Levine, E., Zhang, Z., Kuhlman, T. & Hwa, T. Quantitative characteristics of gene regulation by small RNA. *PLoS Biol.* **5**, e229 (2007).
- Legewie, S., Dienst, D., Wilde, A., Herzel, H. & Axmann, I. M. Small RNAs establish delays and temporal thresholds in gene expression. *Biophys. J.* **95**, 3232–3238 (2008).
- Xiong, W. & Ferrell, J. E. A positive-feedback-based bistable 'memory module' that governs a cell fate decision. *Nature* **426**, 460–465 (2003).
- Ghosh, S. *et al.* Phenotypic heterogeneity in mycobacterial stringent response. *BMC Syst. Biol.* **5**, 18 (2011).
- Berg, O. G., Paulsson, J. & Ehrenberg, M. Fluctuations and quality of control in biological cells: zero-order ultrasensitivity reinvestigated. *Biophys. J.* **79**, 1228–1236 (2000).
- Igoshin, O. A., Price, C. W. & Savageau, M. A. Signalling network with a bistable hysteretic switch controls developmental activation of the F transcription factor in *Bacillus subtilis*. *Mol. Microbiol.* **61**, 165–184 (2006).
- Igoshin, O. A., Brody, M. S., Price, C. W. & Savageau, M. A. Distinctive topologies of partner-switching signaling networks correlate with their physiological roles. *J. Mol. Biol.* **369**, 1333–1352 (2007).

33. Craciun, G., Tang, Y. & Feinberg, M. Understanding bistability in complex enzyme-driven reaction networks. *Proc. Natl Acad. Sci. USA* **103**, 8697–8702 (2006).
34. Thomas, R. & Kaufman, M. Multistationarity, the basis of cell differentiation and memory. I. Structural conditions of multistationarity and other nontrivial behavior. *Chaos* **11**, 170–179 (2001).
35. Klumpp, S., Zhang, Z. & Hwa, T. Growth rate-dependent global effects on gene expression in bacteria. *Cell* **139**, 1366–1375 (2009).
- A re-evaluation of classic microbiology data combined with new theory reveals that the growth rate has widespread consequences for bacterial phenotypes.**
36. Tan, C., Marguet, P. & You, L. Emergent bistability by a growth-modulating positive feedback circuit. *Nature Chem. Biol.* **5**, 842–848 (2009).
- An elegant experimental approach that demonstrates growth-modulated bistability.**
37. Gottesman, S. Proteolysis in bacterial regulatory circuits. *Annu. Rev. Cell Dev. Biol.* **19**, 565–587 (2003).
38. Rotem, E. *et al.* Regulation of phenotypic variability by a threshold-based mechanism underlies bacterial persistence. *Proc. Natl Acad. Sci. USA* **107**, 12541–12546 (2010).
39. Balaban, N. Q., Merrin, J., Chait, R., Kowalik, L. & Leibler, S. Bacterial persistence as a phenotypic switch. *Science* **305**, 1622–1625 (2004).
40. Reed, M. C., Lieb, A. & Nijhout, F. F. The biological significance of substrate inhibition: a mechanism with diverse functions. *Bioessays* **32**, 422–429 (2010).
41. Chaudhury, S. & Ighoshin, O. A. Dynamic disorder-driven substrate inhibition and bistability in a simple enzymatic reaction. *J. Phys. Chem. B* **113**, 13421–13428 (2009).
42. Ighoshin, O. A., Alves, R. & Savageau, M. A. Hysteretic and graded responses in bacterial two-component signal transduction. *Mol. Microbiol.* **68**, 1196–1215 (2008).
43. Ishii, N. *et al.* Multiple high-throughput analyses monitor the response of *E. coli* to perturbations. *Science* **316**, 593–597 (2007).
44. Lynch, M. The frailty of adaptive hypotheses for the origins of organismal complexity. *Proc. Natl Acad. Sci. USA* **104**, 8597–8604 (2007).
45. Rice, S. *Evolutionary Theory* (Sinauer Associates, Inc., 2004).
46. Miyashiro, T. & Goulian, M. High stimulus unmasks positive feedback in an autoregulated bacterial signaling circuit. *Proc. Natl Acad. Sci. USA* **105**, 17457–17462 (2008).
47. Angeli, D., Ferrell, J. E. & Sontag, E. D. Detection of multistability, bifurcations, and hysteresis in a large class of biological positive-feedback systems. *Proc. Natl Acad. Sci. USA* **101**, 1822–1827 (2004).
48. Eguchi, Y., Ishii, E., Hata, K. & Utsumi, R. Regulation of acid resistance by connectors of two-component signal transduction systems in *Escherichia coli*. *J. Bacteriol.* **193**, 1222–1228 (2011).
49. Burton, N. A., Johnson, M. D., Antczak, P., Robinson, A. & Lund, P. A. Novel aspects of the acid response network of *E. coli* K-12 are revealed by a study of transcriptional dynamics. *J. Mol. Biol.* **401**, 726–742 (2010).
- These authors take a detail-oriented experimental approach to evaluating the dynamics of gene-regulatory networks without losing sight of the 'big picture'.**
50. Savageau, M. A. Comparison of classical and autogenous systems of regulation in inducible operons. *Nature* **252**, 546–549 (1974).
51. Traxler, M. F. *et al.* Discretely calibrated regulatory loops controlled by ppGpp partition gene induction across the 'feast to famine' gradient in *Escherichia coli*. *Mol. Microbiol.* **79**, 830–845 (2010).
52. Hoffer, S. M., Westerhoff, H. V., Hellingwerf, K. J., Postma, P. W. & Tommassen, J. Autoamplification of a two-component regulatory system results in "learning" behavior. *J. Bacteriol.* **183**, 4914–4917 (2001).
53. Chastanet, A. *et al.* Broadly heterogeneous activation of the master regulator for sporulation in *Bacillus subtilis*. *Proc. Natl Acad. Sci. USA* **107**, 8486–8491 (2010).
54. Bischofs, I. B., Hug, J. A., Liu, A. W., Wolf, D. M. & Arkin, A. P. Complexity in bacterial cell–cell communication: quorum signal integration and subpopulation signaling in the *Bacillus subtilis* phosphorelay. *Proc. Natl Acad. Sci. USA* **106**, 6459–6464 (2009).
55. Schultz, D., Wolynes, P. G., Jacob, E. & Onuchic, J. N. Deciding fate in adverse times: sporulation and competence in *Bacillus subtilis*. *Proc. Natl Acad. Sci. USA* **106**, 21027–21034 (2009).
56. Saini, S., Ellermeier, J. R., Slauch, J. M. & Rao, C. V. The role of coupled positive feedback in the expression of the SPI1 type three secretion system in *Salmonella*. *PLoS Pathog.* **6**, e1001025 (2010).
57. Thattai, M. & van Oudenaarden, A. Intrinsic noise in gene regulatory networks. *Proc. Natl Acad. Sci. USA* **98**, 8614–8619 (2001).
58. Nguyen, L. K. & Kulasiri, D. On the functional diversity of dynamical behaviour in genetic and metabolic feedback systems. *BMC Syst. Biol.* **3**, 51 (2009).
59. Stekel, D. J. & Jenkins, D. J. Strong negative self regulation of Prokaryotic transcription factors increases the intrinsic noise of protein expression. *BMC Syst. Biol.* **2**, 6 (2008).
60. Goyal, S. & Wingreen, N. S. Growth-induced instability in metabolic networks. *Phys. Rev. Lett.* **98**, 138105 (2007).
61. Bhartiya, S., Chaudhary, N., Venkatesh, K. V. & Doyle, F. J. Multiple feedback loop design in the tryptophan regulatory network of *Escherichia coli* suggests a paradigm for robust regulation of processes in series. *J. R. Soc. Interface* **3**, 383–391 (2006).
62. Curtis, P. D. & Brun, Y. V. Getting in the loop: regulation of development in *Caulobacter crescentus*. *Microbiol. Mol. Biol. Rev.* **74**, 13–41 (2010).
63. Jenal, U. The role of proteolysis in the *Caulobacter crescentus* cell cycle and development. *Res. Microbiol.* **160**, 687–695 (2009).
64. Thanbichler, M. & Shapiro, L. Chromosome organization and segregation in bacteria. *J. Struct. Biol.* **156**, 292–303 (2006).
65. Biondi, E. G. *et al.* Regulation of the bacterial cell cycle by an integrated genetic circuit. *Nature* **444**, 899–904 (2006).
66. Paul, R. *et al.* Allosteric regulation of histidine kinases by their cognate response regulator determines cell fate. *Cell* **133**, 452–461 (2008).
67. Chen, Y. E. *et al.* Spatial gradient of protein phosphorylation underlies replicative asymmetry in a bacterium. *Proc. Natl Acad. Sci. USA* **108**, 1052–1057 (2011).
- An experimentally driven study of the *C. crescentus* cell cycle, making use of mathematical modelling and simulation to circumvent experimental constraints and arrive at a compelling conceptual model.**
68. Hallez, R., Bellefontaine, A.-F., Letesson, J.-J. & De Bolle, X. Morphological and functional asymmetry in  $\alpha$ -proteobacteria. *Trends Microbiol.* **12**, 361–365 (2004).
69. Ackermann, M., Stearns, S. C. & Jenal, U. Senescence in a bacterium with asymmetric division. *Science* **300**, 1920 (2003).
70. Stewart, E. J., Madden, R., Paul, G. & Taddei, F. Aging and death in an organism that reproduces by morphologically symmetric division. *PLoS Biol.* **3**, e45 (2005).
71. Sprinzak, D. & Elowitz, M. B. Reconstruction of genetic circuits. *Nature* **438**, 443–448 (2005).
72. Gardner, T. S., Cantor, C. R. & Collins, J. J. Construction of a genetic toggle switch in *Escherichia coli*. *Nature* **403**, 339–342 (2000).
73. Weiss, R. *Cellular Computation and Communications Using Engineered Genetic Regulatory Networks*. Thesis, Massachusetts Institute of Technology (2001).
74. Atkinson, M. R., Savageau, M. A., Myers, J. T. & Ninfa, A. J. Development of genetic circuitry exhibiting toggle switch or oscillatory behavior in *Escherichia coli*. *Cell* **113**, 597–607 (2003).
75. Elowitz, M. B. & Leibler, S. A synthetic oscillatory network of transcriptional regulators. *Nature* **403**, 335–338 (2000).
76. Yokobayashi, Y., Weiss, R. & Arnold, F. H. Directed evolution of a genetic circuit. *Proc. Natl Acad. Sci. USA* **99**, 16587–16591 (2002).
77. Golding, I., Paulsson, J., Zawilski, S. M. & Cox, E. C. Real-time kinetics of gene activity in individual bacteria. *Cell* **123**, 1025–1036 (2005).
78. Pedraza, J. M. & Paulsson, J. Effects of molecular memory and bursting on fluctuations in gene expression. *Science* **319**, 339–343 (2008).
79. Rosenfeld, N., Young, J. W., Alon, U., Swain, P. S. & Elowitz, M. B. Gene regulation at the single-cell level. *Science* **307**, 1962–1965 (2005).
80. Pedraza, J. M. & van Oudenaarden, A. Noise propagation in gene networks. *Science* **307**, 1965–1969 (2005).
81. Elowitz, M. B., Levine, A. J., Siggia, E. D. & Swain, P. S. Stochastic gene expression in a single cell. *Science* **297**, 1183–1186 (2002).
82. Anderson, J. C., Clarke, E. J., Arkin, A. P. & Voigt, C. A. Environmentally controlled invasion of cancer cells by engineered bacteria. *J. Mol. Biol.* **355**, 619–627 (2006).
83. Basu, S., Mehreja, R., Thiberge, S., Chen, M.-T. & Weiss, R. Spatiotemporal control of gene expression with pulse-generating networks. *Proc. Natl Acad. Sci. USA* **101**, 6355–6360 (2004).
84. Salis, H. M., Mirsky, E. A. & Voigt, C. A. Automated design of synthetic ribosome binding sites to control protein expression. *Nature Biotech.* **27**, 946–950 (2009).
85. Na, D., Lee, S. & Lee, D. Mathematical modeling of translation initiation for the estimation of its efficiency to computationally design mRNA sequences with desired expression levels in prokaryotes. *BMC Syst. Biol.* **4**, 71 (2010).
86. Miyazaki, K. Creating random mutagenesis libraries by megaprimer PCR of whole plasmid (MEGAWHOP). *Methods Mol. Biol.* **231**, 23–28 (2003).
87. Stricker, J. *et al.* A fast, robust and tunable synthetic gene oscillator. *Nature* **456**, 516–519 (2008).
- This article describes the engineering of a robust, tunable synthetic oscillator. The results illustrate the importance of post-transcriptional delays for the dynamic functionality of gene-regulatory networks.**
88. Danino, T., Mondragon-Palmino, O., Tsimring, L. & Hasty, J. A synchronized quorum of genetic clocks. *Nature* **463**, 326–330 (2010).
89. Lim, W. A. Designing customized cell signalling circuits. *Nature Rev. Mol. Cell Biol.* **11**, 393–403 (2010).
90. Martin, V. J. J., Pitera, D. J., Withers, S. T., Newman, J. D. & Keasling, J. D. Engineering a mevalonate pathway in *Escherichia coli* for production of terpenoids. *Nature Biotech.* **21**, 796–802 (2003).
91. Dueber, J. E. *et al.* Synthetic protein scaffolds provide modular control over metabolic flux. *Nature Biotech.* **27**, 753–759 (2009).
- A clever non-transcriptional-modification scheme is shown to greatly boost efficiency in a synthetic metabolic pathway, laying fundamental groundwork for mechanistic synthetic biology.**
92. Keasling, J. D. Synthetic biology for synthetic chemistry. *ACS Chem. Biol.* **3**, 64–76 (2008).
93. Marles-Wright, J. & Lewis, R. J. The stressosome: molecular architecture of a signalling hub. *Biochem. Soc. Trans.* **38**, 928–933 (2010).
94. Marles-Wright, J. *et al.* Molecular architecture of the "stressosome," a signal integration and transduction hub. *Science* **322**, 92–96 (2008).
95. Lovdok, L. *et al.* Role of translational coupling in robustness of bacterial chemotaxis pathway. *PLoS Biol.* **7**, e1000171 (2009).
96. Saiz, L. & Vilar, J. M. J. *Ab initio* thermodynamic modeling of distal multisite transcription regulation. *Nucleic Acids Res.* **36**, 726–731 (2008).
97. Long, T. *et al.* Quantifying the integration of quorum-sensing signals with single-cell resolution. *PLoS Biol.* **7**, e1000668 (2009).
98. Feinberg, M. The existence and uniqueness of steady states for a class of chemical reaction networks. *Arch. Rational Mech. Anal.* **132**, 311–370 (1995).
99. Shinar, G. & Feinberg, M. Structural sources of robustness in biochemical reaction networks. *Science* **327**, 1389–1391 (2010).
100. Batchelor, E. & Goulian, M. Robustness and the cycle of phosphorylation and dephosphorylation in a two-component regulatory system. *Proc. Natl Acad. Sci. USA* **100**, 691–696 (2003).
101. Shinar, G., Milo, R., Martínez, M. R. & Alon, U. Input output robustness in simple bacterial signaling systems. *Proc. Natl Acad. Sci. USA* **104**, 19931–19935 (2007).

### Acknowledgements

The authors thank G. Balázs, M. Laub, M. Bennett and M. Gennaro for useful comments on manuscript drafts and P. Lund for sharing his data for figure 4. This work is supported by grant R01-GM096189-01 from the US National Institutes of Health (O.A.I.).

### Competing interests statement

The authors declare no competing financial interests.

### FURTHER INFORMATION

Oleg A. Ighoshin's homepage: <http://igoshin.rice.edu>

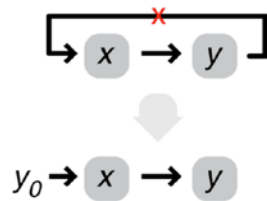
### SUPPLEMENTARY INFORMATION

See online article: [S1](#) (box)

ALL LINKS ARE ACTIVE IN THE ONLINE PDF

Supplementary information S1 (box)

One method to understand feedback is to “break the loop,” turning the closed-loop feedback system into one with a defined input and output. In the resulting open-loop system, the output would feed back into the input. In the following system, we break the loop in a system with an output  $y$  that feeds back into  $x$ :



We can then measure the sign and strength of the now-broken feedback loop with the concept of sensitivity: how much the output  $y$  changes for a small change in the input ( $y_0$ ). In this particular case, the sensitivity is called an open-loop gain because it measures the gain (or how much  $y$  changes with respect to changes in  $y_0$ ) of the open-loop form of the closed-loop system. Mathematically, sensitivity of  $y$  to changes in the point of feedback regulation ( $y_0$ ) at a given steady state ( $x, y$ ) is calculated with the formula:

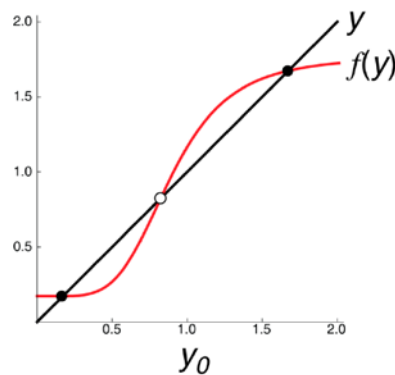
$$\gamma = \left. \frac{\partial y}{\partial y_0} \right|_{y_0 = \hat{y}}$$

The sign of  $\gamma$  tells us the sign of feedback. Note that the sign of feedback may not be obvious, and may emerge from complex interactions in the network that connects  $x$  to  $y$ .

For instance, we can find the open-loop gain in a simple mathematical model of a two-component system (FIG. 1), by defining mathematical forms with one or more rate constant for each process embedded in the system. Sparing the details of computation, we found that  $\gamma$  is proportional to  $k_{pr}k_d - k_{ph}k_e$  where  $k_{pr}$  and  $k_{ph}$  are respective rates of regulator phosphorylation and dephosphorylation by the sensor,  $k_d$  is the rate of dilution from growth, and  $k_e$  is the rate parameter for exogenous phosphorylation. This simple relationship between the gain and rate constants tells us several things about transcriptional feedback in two-component systems:

- (i) regulator dephosphorylation and exogenous phosphorylation are both necessary for negative feedback and thus overshoot kinetics;
- (ii) because the dilution rate  $k_d$  is small even for fast exponential growth, the rate of exogenous phosphorylation can be small and still permit negative feedback;
- (iii) different magnitudes of external signalling that modulate phosphorylation and dephosphorylation of the regulator via the sensor ( $k_{pr}$  or  $k_{ph}$ ) can result in different effective feedback signs.

If the circuit diagram of a network (BOX 2) has only unambiguously *positive* feedback loops, and its open-loop form has a single steady state, breaking the loop can determine if the intact system is bistable<sup>47</sup>. The basic idea is to use the open-loop form of the system to quantify  $y$  at steady state as a function of  $y_0$ . We denote this function, the open-loop characteristic curve, by  $f(y_0)$ . Then graph  $y = f(y_0)$  along with the feedback strength of the system (that is, open-loop gain, here for simplicity  $y_0 = y$ ) and look for intersections:



If the system is bistable as in the graph above, the system will have two stable steady states (black points) and one unstable (open circle).